

ESTIMATING THE AVERAGE SIZE OF FIBER/MATRIX INTERFACE CRACKS IN UD AND CROSS-PLY LAMINATES

L. Di Stasio^{1,2}, J. Varna¹, Z. Ayadi²

¹ Division of Materials Science, Luleå University of Technology, Luleå, Sweden

²EEIGM & IJL, Université de Lorraine, Nancy, France

Grupo de Elasticidad y Resistencia de Materiales, ETSI Sevilla
Sevilla (ES) - September , 2019



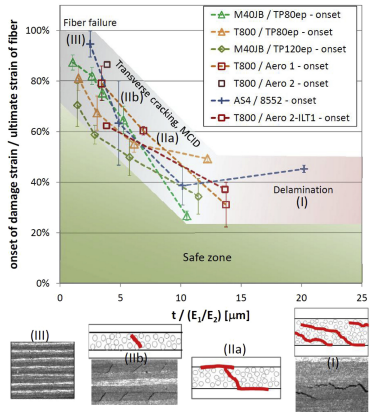
Outline



INITIATION OF TRANSVERSE CRACKS IN THIN-PLIES

The Thin-ply “Advantage”: new material

2018, $[45^\circ, 90^\circ, -45^\circ, 0^\circ]$ ns

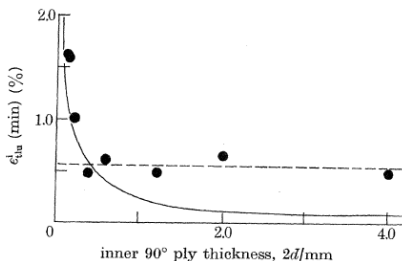
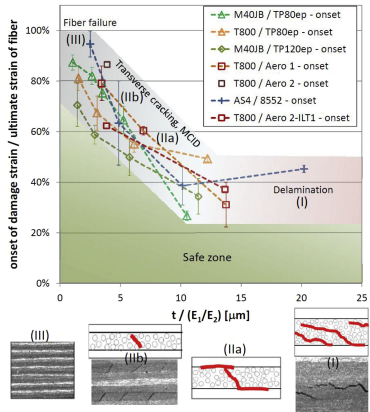


Cugnoni et al., Compos. Sci. Technol. **168**, 2018.

The Thin-ply “Advantage”: new material, old result

2018, $[45^\circ, 90^\circ, -45^\circ, 0^\circ]_{nS}$

1979, $[0^\circ, 90^\circ]_S$



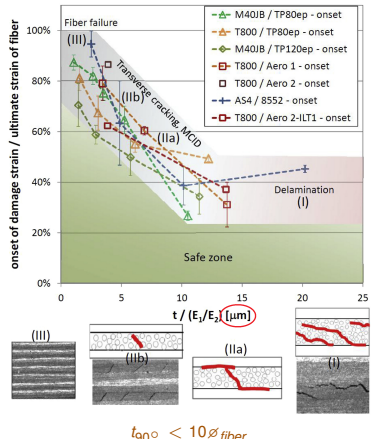
Cugnoni et al., Compos. Sci. Technol. **168**, 2018.

Bailey et al., P. Roy. Soc. A-Math. Phy. **366** (1727), 1979.

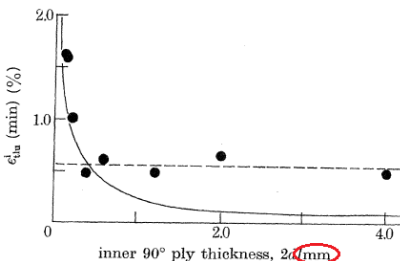
The Thin-ply “Advantage”: new material, old result?

2018, $[45^\circ, 90^\circ, -45^\circ, 0^\circ]_{nS}$

1979, $[0^\circ, 90^\circ]_S$



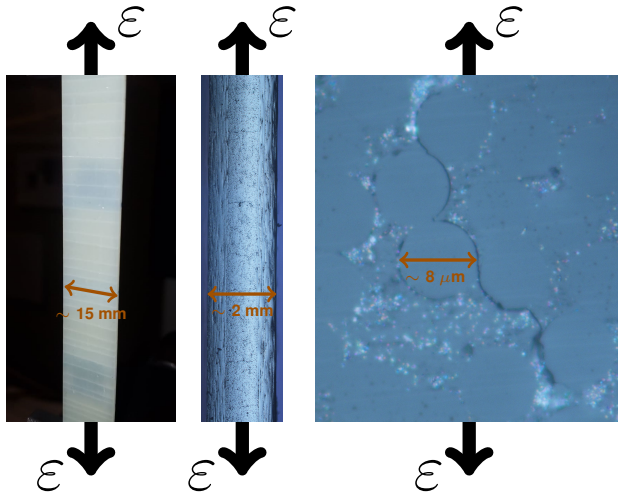
Cugnoni et al., Compos. Sci. Technol. **168**, 2018.



$t_{90^\circ} > 100\phi_{fiber}$

Bailey et al., P. Roy. Soc. A-Math. Phys. **366** (1727), 1979.

Micromechanics of Initiation



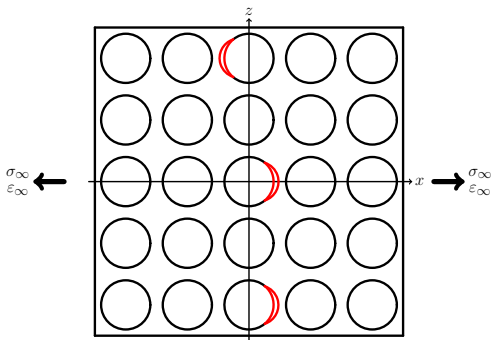
Left:
front view of $[0, 90]_S$,
visual inspection.

Center:
edge view of $[0, 90]_S$,
optical microscope.

Right:
edge view of $[0, 90]_S$,
optical microscope.

Micromechanics of Initiation

Stage 1: isolated debonds



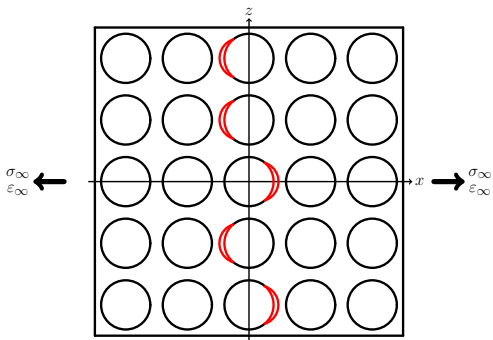
Bailey et al., P. Roy. Soc. A-Math. Phy. **366** (1727), 1979.

Bailey et al., J. Mater. Sci. **16** (3), 1981.

Zhang et al., Compos. Part A-Appl. S. **28** (4), 1997.

Micromechanics of Initiation

Stage 2: consecutive debonds



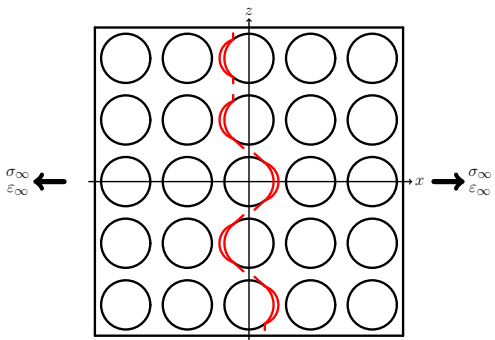
Bailey et al., P. Roy. Soc. A-Math. Phy. **366** (1727), 1979.

Bailey et al., J. Mater. Sci. **16** (3), 1981.

Zhang et al., Compos. Part A-Appl. S. **28** (4), 1997.

Micromechanics of Initiation

Stage 3: kinking



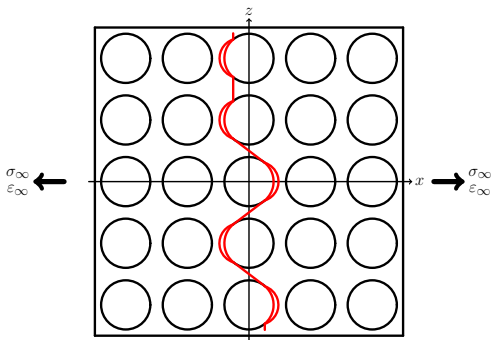
Bailey et al., P. Roy. Soc. A-Math. Phy. **366** (1727), 1979.

Bailey et al., J. Mater. Sci. **16** (3), 1981.

Zhang et al., Compos. Part A-Appl. S. **28** (4), 1997.

Micromechanics of Initiation

Stage 4: coalescence



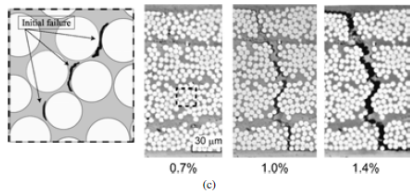
Bailey et al., P. Roy. Soc. A-Math. Phy. **366** (1727), 1979.

Bailey et al., J. Mater. Sci. **16** (3), 1981.

Zhang et al., Compos. Part A-Appl. S. **28** (4), 1997.

A Counter-intuitive Observation

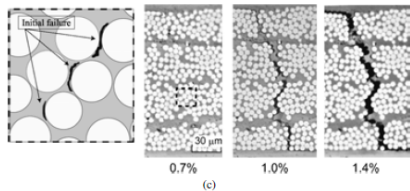
$[0^\circ, 90^\circ]_S$



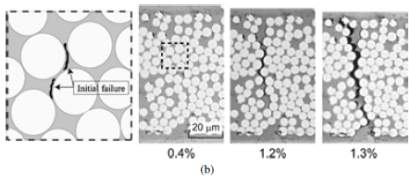
$$n = 4, t_{90^\circ} = 160 \mu m$$

A Counter-intuitive Observation

$[0^\circ, 90^\circ]_S$



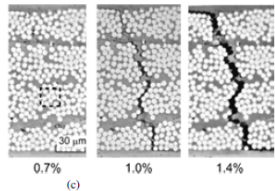
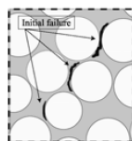
$$n = 4, t_{90^\circ} = 160 \mu m$$



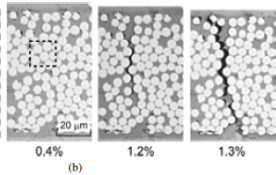
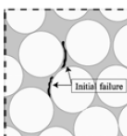
$$n = 2, t_{90^\circ} = 80 \mu m$$

A Counter-intuitive Observation

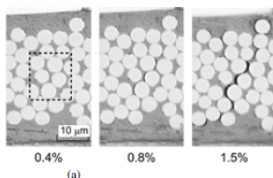
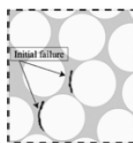
$[0^\circ, 90^\circ]_S$



$n = 4, t_{90^\circ} = 160 \mu m$



$n = 2, t_{90^\circ} = 80 \mu m$



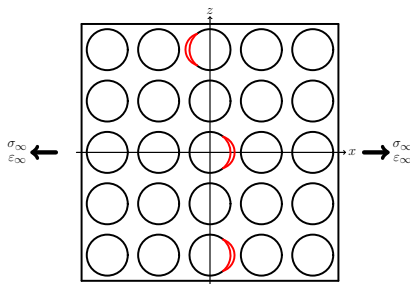
$n = 1, t_{90^\circ} = 40 \mu m$

Saito et al., Adv. Compos. Mater. 21 (1), 2012.

Objective of the Study

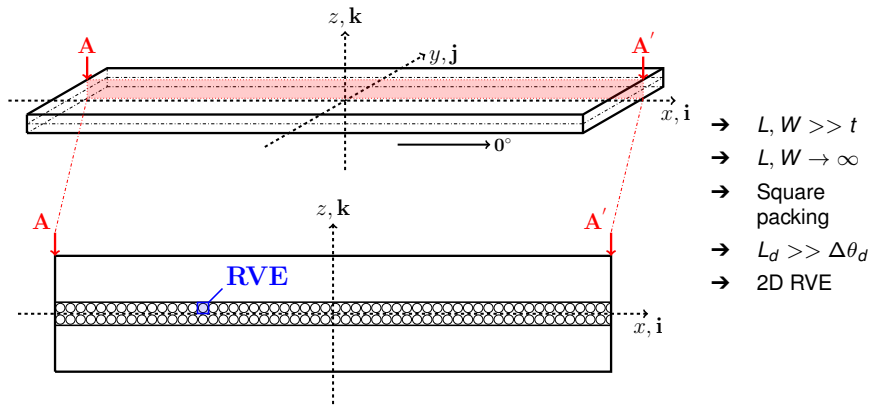
Can we talk about a ply-thickness effect for the fiber-matrix interface crack?

Stage 1: isolated debonds

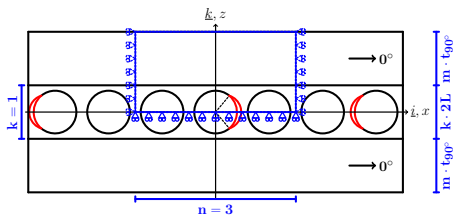


MODELING

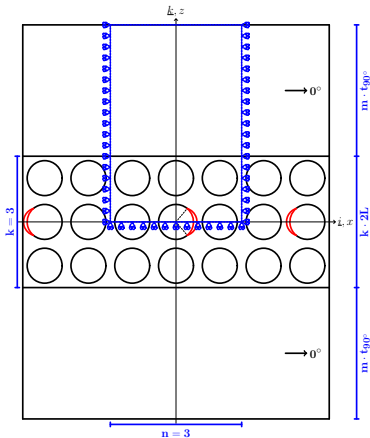
Geometry



Representative Volume Elements

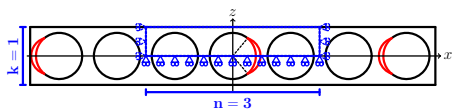


$$n \times 1 - m \cdot t_{90^\circ}$$

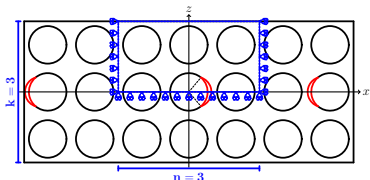


$$n \times k - m \cdot t_{90^\circ}$$

Representative Volume Elements

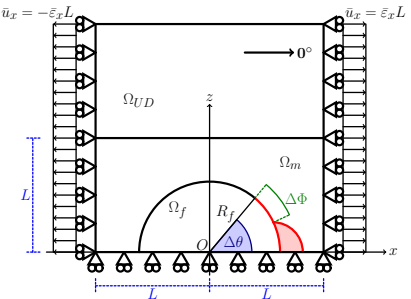


– free
 $n \times 1 - \text{coupling}$
– coupling + H



– free
 $n \times k - \text{coupling}$
– coupling + H

Assumptions

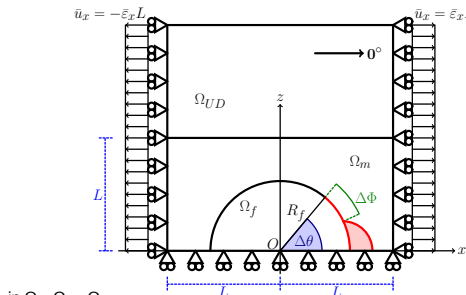


- Linear elastic, homogeneous materials
- Concentric Cylinders Assembly with Self-Consistent Shear Model for UD
- Plane strain
- Frictionless contact interaction
- Symmetric w.r.t. x-axis
- Coupling of x-displacements on left and right side (repeating unit cell)
- Applied uniaxial tensile strain $\bar{\varepsilon}_x = 1\%$
- $V_f = 60\%$

$$R_f = 1 \text{ } [\mu\text{m}] \quad L = \frac{R_f}{2} \sqrt{\frac{\pi}{V_f}}$$

Material	V_f [%]	E_L [GPa]	E_T [GPa]	μ_{LT} [GPa]	ν_{LT} [-]	ν_{TT} [-]
Glass fiber	-	70.0	70.0	29.2	0.2	0.2
Epoxy	-	3.5	3.5	1.25	0.4	0.4
UD	60.0	43.442	13.714	4.315	0.273	0.465

Solution



in Ω_f , Ω_m , Ω_{UD} :

$$\frac{\partial^2 \varepsilon_{xx}}{\partial x^2} + \frac{\partial^2 \varepsilon_{zz}}{\partial z^2} = \frac{\partial^2 \gamma_{zx}}{\partial x \partial z} \quad \text{for } 0^\circ \leq \alpha \leq \Delta\theta :$$

$$\varepsilon_V = \gamma_{xx} = \gamma_{yz} = 0$$

for $\Delta\theta < \alpha < 180^\circ$:

$$\frac{\partial \sigma_{xx}}{\partial x} + \frac{\partial \tau_{zx}}{\partial z} = 0$$

$$\vec{U}_m(R_f, \alpha) = \vec{U}_f(R_f, \alpha) = 0$$

$$\frac{\partial x}{\partial \sigma} = \frac{\partial z}{\partial \sigma}$$

$$\sigma_{ij} = E_{ijkl}\varepsilon_{kl}$$

$$\frac{\partial \tau_{zx}}{\partial x} + \frac{\partial \sigma_{zz}}{\partial z} = 0$$

+ BC

$$\sigma_{yy} = \nu (\sigma_{xx} + \sigma_{zz})$$

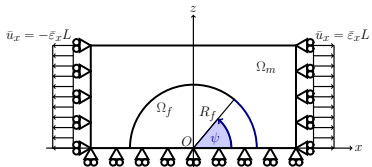
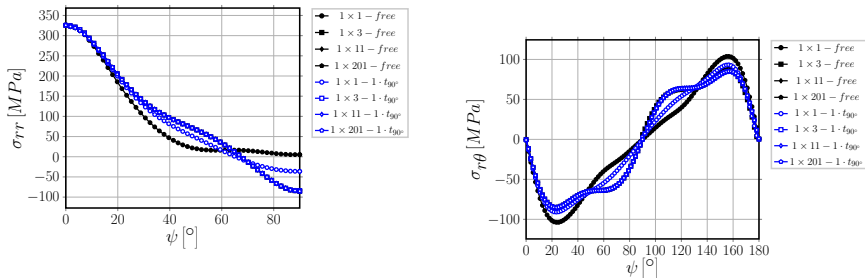
- oscillating singularity
$$\sigma \sim r^{-\frac{1}{2}} \sin(\varepsilon \log r), \quad V_f \rightarrow 0$$

$$\varepsilon = \frac{1}{2\pi} \log \left(\frac{1-\beta}{1+\beta} \right)$$

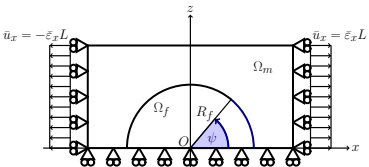
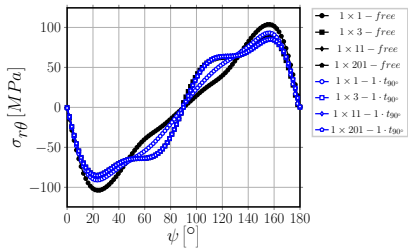
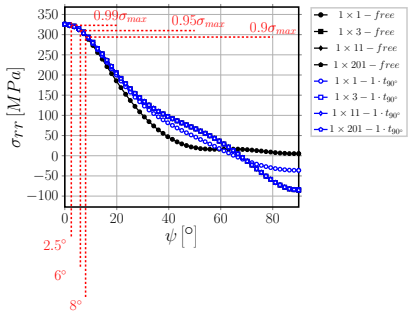
$$\beta = \frac{\mu_2(\kappa_1 - 1) - \mu_1(\kappa_2 - 1)}{\mu_2(\kappa_1 + 1) + \mu_1(\kappa_2 + 1)}$$
 - receding contact
 - $\frac{G(R_{f,2})}{G(R_{f,1})} = \frac{R_{f,2}}{R_{f,1}}, \quad \frac{G(\bar{\varepsilon}_{x,2})}{G(\bar{\varepsilon}_{x,1})} = \frac{\bar{\varepsilon}_{x,2}^2}{\bar{\varepsilon}_{x,1}^2}$
 - FEM + LEFM (VCCT)
 - 2nd order shape functions
 - regular mesh of quadrilaterals at the crack tip:
 - $AR \sim 1, \quad \delta = 0.05^\circ$

DEBOND INITIATION

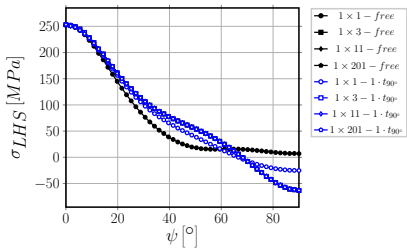
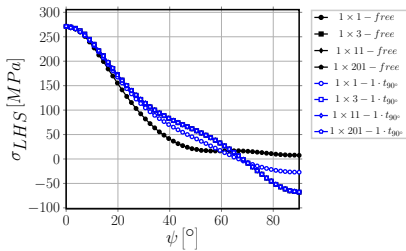
σ_{rr} vs $\tau_{r\theta}$: radial stress vs tangential shear at the interface



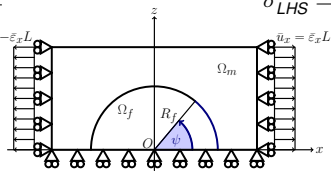
σ_{rr} vs $\tau_{r\theta}$: radial stress vs tangential shear at the interface



σ_{LHS} : local hydrostatic stress at the interface

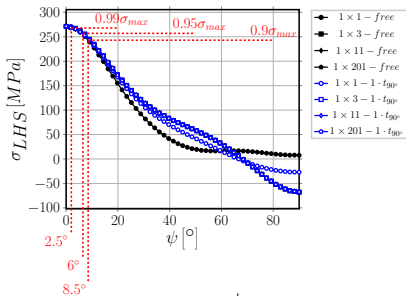


$$\sigma_{LHS}^{2D} = \frac{\sigma_{rr} + \sigma_{\theta\theta}}{2}$$

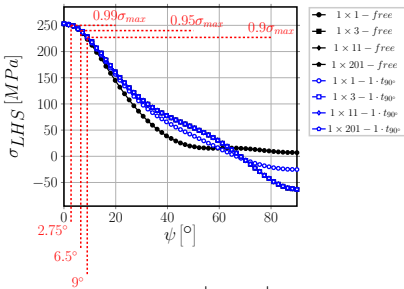
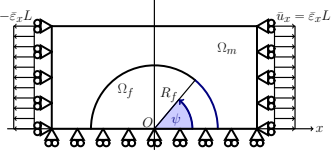


$$\sigma_{LHS}^{3D} = \frac{\sigma_{rr} + \sigma_{\theta\theta} + \sigma_{yy}}{3}$$

σ_{LHS} : local hydrostatic stress at the interface

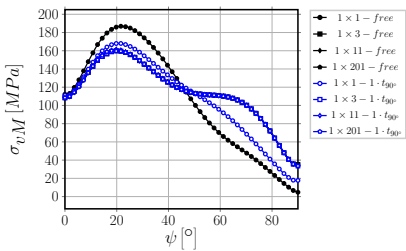
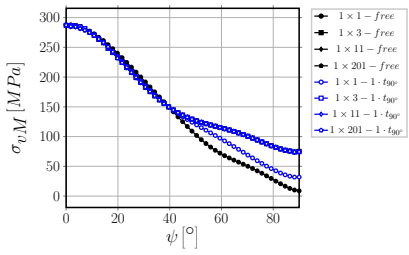


$$\sigma_{LHS}^{2D} = \frac{\sigma_{rr} + \sigma_{\theta\theta}}{2}$$



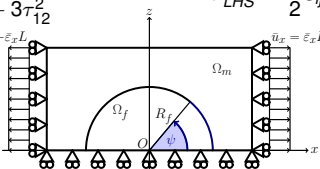
$$\sigma_{LHS}^{3D} = \frac{\sigma_{rr} + \sigma_{\theta\theta} + \sigma_{yy}}{3}$$

σ_{vM} : von Mises stress at the interface



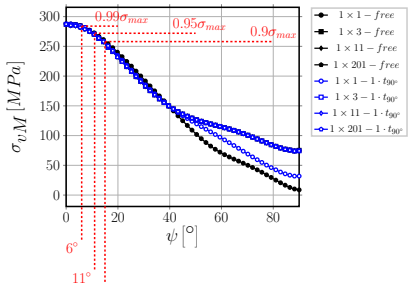
$$\sigma_{vM}^{2D} = \sqrt{(\sigma_{rr} - \sigma_{\theta\theta})^2 + 3\tau_{12}^2}$$

$$\bar{u}_x = -\bar{\varepsilon}_x L$$

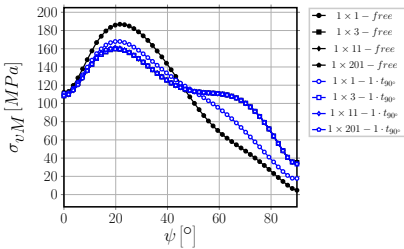


$$\sigma_{LHS}^{3D} = \frac{3}{2} s_{ij} s_{ij} \quad s_{ij} = \sigma_{ij} - \frac{1}{3} \sigma_{kk} \delta_{ij}$$

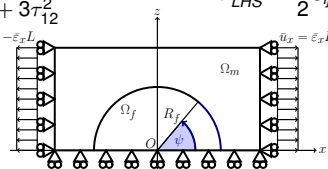
σ_{vM} : von Mises stress at the interface



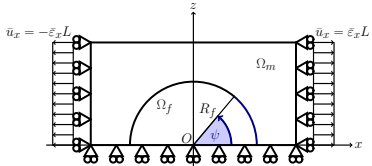
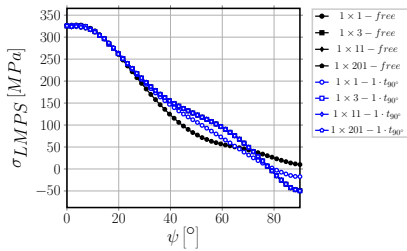
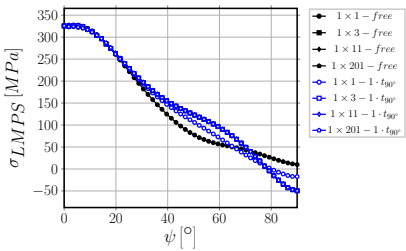
$$\sigma_{vM}^{2D} = \sqrt{(\sigma_{rr} - \sigma_{\theta\theta})^2 + 3\tau_{12}^2}$$



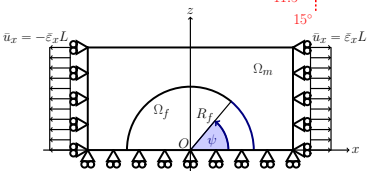
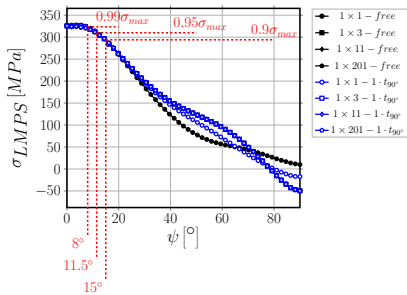
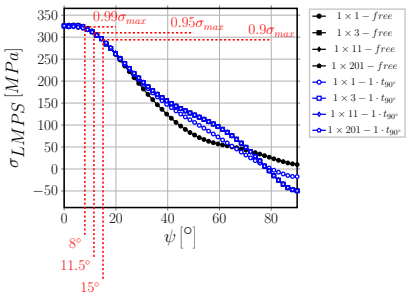
$$\sigma_{LHS}^{3D} = \frac{3}{2} s_{ij} s_{ij} \quad s_{ij} = \sigma_{ij} - \frac{1}{3} \sigma_{kk} \delta_{ij}$$



σ_I : maximum principal stress at the interface



σ_I : maximum principal stress at the interface

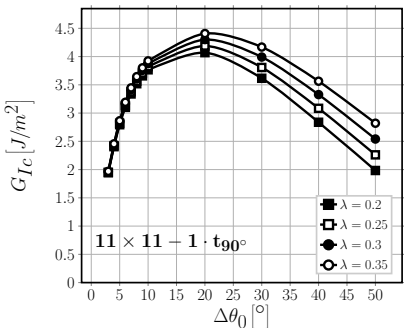
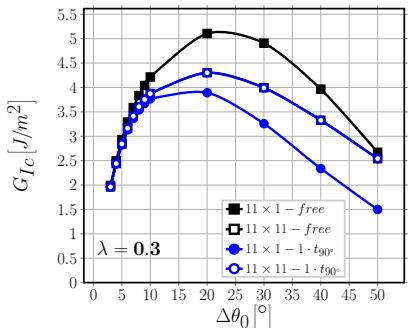


Summary



DEBOND PROPAGATION

Estimation of G_{lc}

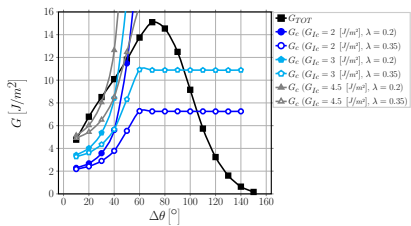


$$G_{lc} = \frac{G_c}{1 + \tan^2((1 - \lambda) \Psi_G)} \Big|_{G_c=G_{TOT}(\Delta\theta_0)},$$

$$\Psi_G = \tan^{-1} \left(\sqrt{\frac{G_{II}}{G_I}} \right) \Big|_{\Delta\theta_0}$$

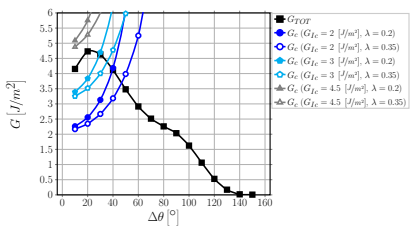
Estimation of $\Delta\theta_{max}$

$21 \times 1 - free$



$$\Delta\theta_{max} \in (30^\circ - 105^\circ)$$

$21 \times 1 - 1 \cdot t_{90^\circ}$

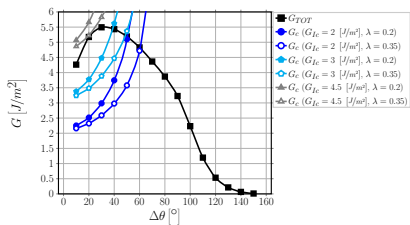


$$\Delta\theta_{max} \in (30^\circ - 50^\circ)$$

$$G_{TOT}(\Delta\theta) > G_c = G_{Ic} \left(1 + \tan^2((1-\lambda)\Psi_G) \right), \quad \Psi_G = \tan^{-1} \left(\sqrt{\frac{G_{II}}{G_I}} \right) \Big|_{\Delta\theta}$$

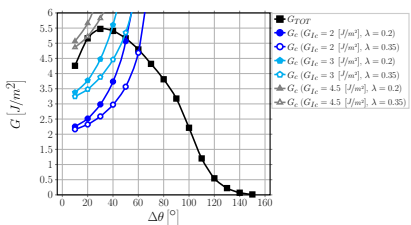
Estimation of $\Delta\theta_{max}$

$21 \times 3 - free$



$$\Delta\theta_{max} \in (40^\circ - 60^\circ)$$

$21 \times 3 - 1 \cdot t_{90^\circ}$

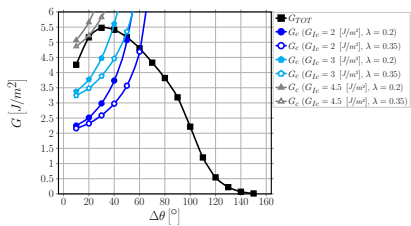


$$\Delta\theta_{max} \in (40^\circ - 60^\circ)$$

$$G_{TOT}(\Delta\theta) > G_c = G_{Ic} \left(1 + \tan^2((1-\lambda)\Psi_G) \right), \quad \Psi_G = \tan^{-1} \left(\sqrt{\frac{G_{II}}{G_I}} \right) \Big|_{\Delta\theta}$$

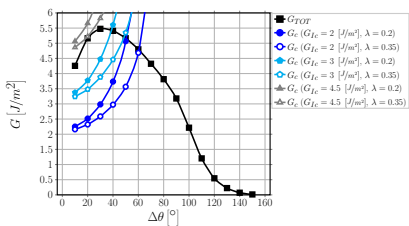
Estimation of $\Delta\theta_{max}$

$21 \times 21 - free$



$$\Delta\theta_{max} \in (40^\circ - 60^\circ)$$

$21 \times 21 - 1 \cdot t_{90}$

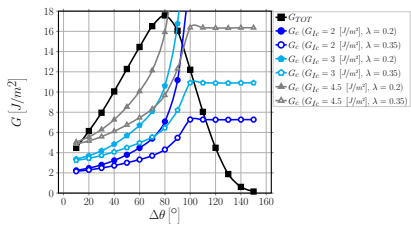


$$\Delta\theta_{max} \in (40^\circ - 60^\circ)$$

$$G_{TOT}(\Delta\theta) > G_c = G_{Ic} \left(1 + \tan^2((1-\lambda)\Psi_G) \right), \quad \Psi_G = \tan^{-1} \left(\sqrt{\frac{G_{II}}{G_I}} \right) \Big|_{\Delta\theta}$$

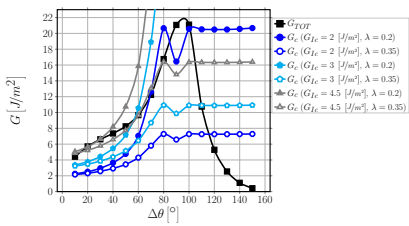
Estimation of $\Delta\theta_{max}$

$21 \times 21 - symm$



$$\Delta\theta_{max} \in (80^\circ - 110^\circ)$$

$21 \times 21 - asymm$



$$\Delta\theta_{max} \in (55^\circ - 115^\circ)$$

$$G_{TOT}(\Delta\theta) > G_c = G_{lc} \left(1 + \tan^2((1-\lambda)\Psi_G) \right), \quad \Psi_G = \tan^{-1} \left(\sqrt{\frac{G_{II}}{G_I}} \right) \Big|_{\Delta\theta}$$

CONCLUSIONS

Conclusions

- No effect of 90° ply thickness can be observed when t_{90° is at least $\sim 3\phi_{fiber}$
- Only if t_{90° is reduced to $1\phi_{fiber}$, ERR is reduced for a given level of applied strain, i.e. debond growth is delayed to higher levels of applied strain ($G \sim \varepsilon_{applied}^2$)
- No effect of 0° ply thickness can be observed when $t_{0^\circ}/t_{90^\circ} > 1$
- A small difference can be observed when $t_{0^\circ} = t_{90^\circ}$, due to the smaller bending stiffness of a thinner 0° layer

